ACS OMEGA

Open Access

http://pubs.acs.org/journal/acsodf

Article

First-Principles Structure Search Study of 17-β-Estradiol Adsorption on Graphene

Saara Sippola, Milica Todorović,* and Emilia Peltola*

Cite This: *ACS Omega* 2024, 9, 34684−34691

Read Online

ACCESS | Metrics & More | Article Recommendations

ABSTRACT: 17-Beta-estradiol (E2), a steroid hormone synthesized from cholesterol, has various impacts on health and the environment. Currently, the gold standard for its measurement in the body is a conventional blood test (mass spectrometry), but carbon-based electrochemical sensors have been proposed as an alternative due to their advantages, such as rapid analysis time and sensitivity. To improve the atomic-level understanding of the interactions at the substrate surface, we performed density functional theory (DFT) simulations to study the nature of the adsorption of E2 on pristine graphene. Bayesian Optimization Structure Search (BOSS) was employed to reduce human bias in the determination of the most favorable adsorption configurations. Two stable adsorption minimum configurations were found. Analysis of their electronic properties indicates that E2 physisorbs on graphene. Embarking upon complex carbonaceous materials, the importance of finding all possible minimum candidates with automated structure search tools is highlighted. Computational investigations facilitate tailoring substrate materials with outstanding performance and applications in neuroscientific research, fertility monitoring, and clinical trials. Combining them with experimental research carries significant potential to advance sensor design beyond the current state-of-the-art.

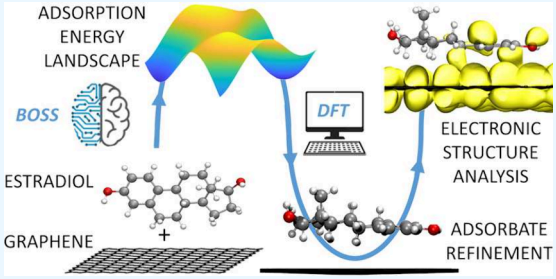

INTRODUCTION

17-Beta-estradiol (E2) is a steroid hormone best known for its role in the menstrual cycle and the development of female secondary sexual characteristics. However, in recent decades, its various other impacts on health and the environment have drawn a lot of interest. E2 regulates synaptic plasticity, which is essential for learning and memory,[1,2] influences social interactions,[3] and is a major endocrine-disrupting chemical (EDC) due to its widespread medical use.[4,5] In addition, E2 and other hormones that fluctuate during the menstrual cycle affect female metabolism, which leads to misestimated medication doses and side effects due to the under-representation of women in clinical trials.[6,7] All E2 is synthesized from cholesterol, and most of it is secreted by the ovaries, adrenal cortex, and fat tissue. Additionally, E2 is secreted locally in the brain by neurons and, following a brain injury, also by a type of neural supporting cell (astrocytes), which indicates it might have a neuroprotective role.[8]

To study the role of E2 in our bodies, measurement tools that detect minimal changes in its concentration (sensitivity) and effectively differentiate it from interferents (selectivity) are required. The low concentration of E2 in the solutions of interest poses its challenge: a detection limit as low as 0.2−0.4 ng/L would be beneficial to measure E2 in blood and wastewaters.[9,10] Today, the most sophisticated way of measuring the concentration of E2 in blood is a conventional, invasive, and labor-intensive blood test. While it offers standardized protocols, it is slow and expensive because it requires lab analysis by trained personnel and costly equipment. It also does not allow rapid in vivo measurements that are required to study the functions of E2 in the brain. Unsurprisingly, current research is primarily focused on measuring of E2 in environmental samples.[11]

Electrochemical sensors, where E2 is detected directly at the substrate via oxidation,[12−14] have been proposed as an alternative to conventional methods due to their several advantages, such as sensitivity, cost-effectiveness, rapid analysis time, and a smaller sample volume. Compared to biosensors, where the detection happens via eroding biorecognition elements, direct electrochemical sensing technologies allow developing sensors with longer life spans. Carbon-based hybrid nanomaterials have been shown to outperform state-of-the-art materials like gold and platinum in sensing substrates.[15] However, the experimental development of sensor materials currently relies heavily on trial-and-error methods, raising questions about resource optimization. To enhance sensor

Received: April 11, 2024
Revised: July 19, 2024
Accepted: July 25, 2024
Published: August 3, 2024

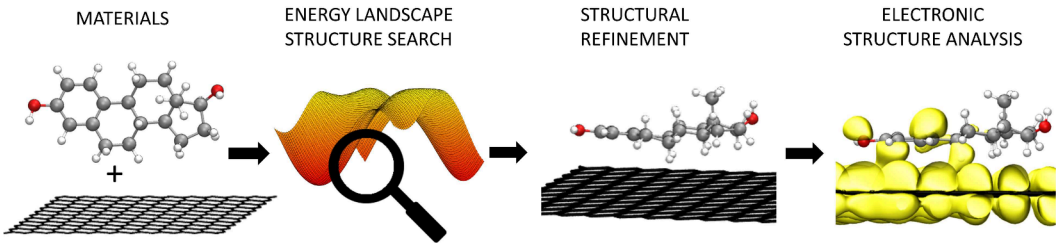

Figure 1. Workflow for determining the optimal adsorption configurations of 17-beta-estradiol on pristine graphene.

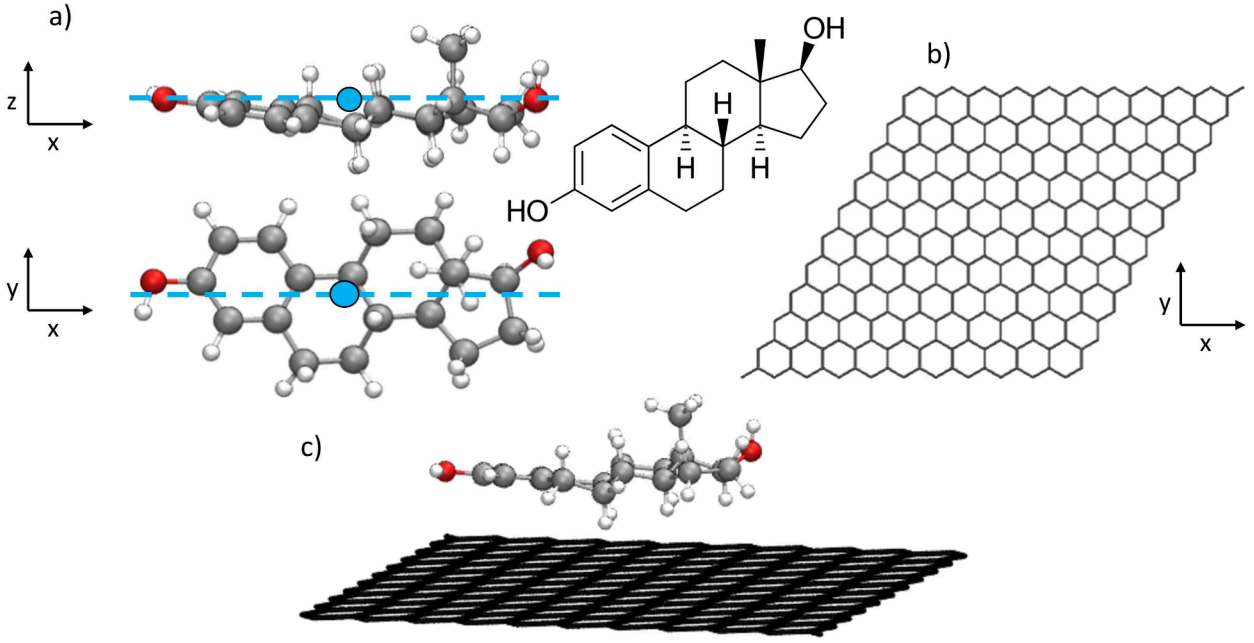

Figure 2. Components of the system. (a) Structural formula and optimized standalone configuration of E2 in top-view and side-view. The dashed lines mark the long axis of the molecule, and the circles denote the location of its center of mass. (b) Optimized standalone configuration of the 11 × 11 graphene supercell. (c) E2 placed on top of the graphene supercell.

design, there is a need for a rational approach driven by an atomic-level understanding of the interactions at the substrate surface. This facilitates tailoring the sensors for desired applications with outstanding performance (sensitivity and selectivity).

Evidence suggests that the interactions of E2 on carbon-fiber surfaces are adsorption-controlled, making successful adsorption a precondition for the optimal detection of E2.[11,16] Previously, only one manuscript reporting computational results on the adsorption of E2 on graphene has been published.[17] Additionally, the adsorption of E2 on graphene oxide has been studied using density functional theory (DFT) and classical molecular dynamics.[18,19] In each paper, the authors exclusively rely on chemical intuition to determine candidate adsorption configurations.

In this Article, we perform DFT simulations to study the nature of adsorption of E2 on a pure graphene substrate. To reduce human bias in the determination of candidate adsorption minimum structures, we employ Bayesian Optimization Structure Search (BOSS), a novel active learning method, which utilizes Bayesian optimization to sample the adsorption energy surface with reduced computational costs compared to dense single-point DFT calculations.[20,21] Figure 1 describes the workflow of the study, starting from system construction, continuing to structure search and refinement, and finally, the analysis of the results. Due to the significance of adsorption to E2 detection and the role of graphene as a building block (BB) for many complex carbon-based nanomaterials, this study marks a preliminary step in building an understanding of the interactions between E2 and carbon-based nanomaterials.

In this Article, our objectives are to identify the stable adsorption minima of E2 on pristine graphene and to detect the presence of any covalent bonds. Understanding the adsorption process thoroughly will enhance the development of novel carbon-based sensor materials for E2 detection. Electrochemical sensors for E2 have a plethora of interesting use cases in clinical trials, fertility monitoring, and neuroscientific research.

METHODS

To identify the most favorable adsorption configurations of E2 on pristine graphene, we followed the well-established BOSS workflow from previous organic surface adsorption studies.[20,22−24] The workflow involves: (a) molecule and substrate model preparation, (b) a BO-guided configurational adsorbate search, (c) detection of optimal configurations based on their adsorption energy, (d) their structural refinement, and (e) electronic structure analysis.

Computational Details. We employed FHI-Aims (version 200112.2) for all DFT calculations.[25] Light default settings

https://doi.org/10.1021/acsomega.4c03485
ACS Omega 2024, 9, 34684−34691

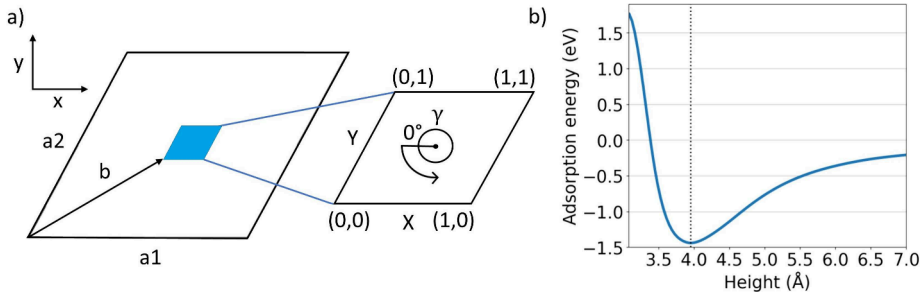

Figure 3. Results of the 1D BOSS search and degrees of freedom for the 3D BOSS search. (a) Location of the unit cell on the 11 × 11 graphene supercell and search boundaries of the 3D BOSS search. (b) Adsorption energy (eV) as a function of the height (Å) of the molecule from the surface.

with tier 1 basis sets were used in the structure search, and tight default settings with tier 2 basis sets were used for model refinement and electronic structure calculations. The generalized-gradient approximation of Perdew−Burke−Ernzerhof (PBE)[26] was chosen as an exchange-correlation functional, and the semiclassical Thatchenko−Scheffler method was applied for van der Waals (vdW) corrections.[27] All calculations were performed spin unpolarized, and the value of Gaussian broadening was set to 0.1 eV. A 2 × 2 × 1 k-grid and a dipole correction were employed. The total energy was converged below 10^{-6} eV, and the relaxation of structures was defined by maximum residual force component below 10^{-2} eV/Å. For density of states (DOS) calculations, a denser 6 × 6 × 1 k-grid and 100 energy data points per eV were used.

We prepared the molecule and surface models separately in the gas phase. E2 is a conjugated aromatic molecule with a nearly flat backbone that consists of a phenolic ring, two cyclohexanes, and a cyclopentane. The two end groups are hydroxyls, and the methyl group is attached to a connecting point between the cyclopentane and one of the cyclohexanes. In the bloodstream, pH levels of ca. 7.4 are below those required for E2 deprotonation, so we simulated E2 in its neutral form. The 44-atom molecule model structure was built using Avogadro software (version 1.2.0)[28,29] and preoptimized with a classical force field before the full optimization with DFT. For the pristine graphene model, we selected a structure from a previous study.[30] Here, the graphene 1 × 1 lattice constant is 2.465 Å, and the C−C bond length is 1.42 Å in accordance with previous knowledge.[31,32] To accommodate the E2 molecule, we utilized an 11 × 11 graphene supercell (lattice vectors a_1 = [27.111, 0, 0] and a_2 = [13.555, 23.478, 0]), with a vertical cell height of 50 Å. To avoid edge effects, graphene was modeled as an infinite layer with periodic boundary conditions instead of a nanoflake model. The axes were defined as follows: x = [1, 0, 0], y = [0, 1, 0], and z= [0, 0, 1]. The components of the system are described in Figure 2.

The obtained total energies were used to calculate the adsorption energies of the chosen minimum configurations. All adsorption energies were calculated using the formula

$$E_{ADS} = E_{TOT} - (E_{GR} + E_{E2})$$

where E_{TOT} is the total energy of the combined system, E_{GR} is the total energy of the relaxed, isolated 11 × 11 graphene sheet, and E_{E2} is the total energy of the relaxed, isolated E2 molecule.

BOSS Structure Search. In the configurational adsorbate search, we kept the substrate fixed and varied the position and orientation of the molecule above the surface. At this stage, the molecule and substrate models were kept rigid to reduce search complexity. We consider the approximation adequate for these materials, given that both the molecule and substrate are planar, electronically conjugated systems and only minor deformations are expected after adsorption. Since benzene is well-known to adsorb horizontally on graphene substrates due to $\pi-\pi$ stacking[33,34] and similar behavior has been found for a catechol structure dopamine,[35] we expect E2 to also adsorb horizontally to pristine graphene. We excluded from consideration E2 tilting toward the substrate along the long and short molecular axes, but the registry and orientation of the adsorbed molecule with respect to the substrate remained unclear. The configurational search was performed in the remaining four dimensions (4D): the position of the molecule above the surface (x, y, z) and the γ-angle of in-plane rotation of E2 with respect to the z-axis (perpendicular to the substrate).

The molecule was originally oriented to place the conjugated backbone parallel to the substrate, with its long and short axes aligned with the x- and y-coordinate axes. The E2 position was described by the molecular center of mass (COM). Because of the high periodicity of pristine graphene, it was sufficient to limit the $x-y$ registry search to a single surface unit of the supercell, with the lattice vectors a_1 = [2.465, 0, 0] and a_2 = [1.232, 2.134, 0]. To avoid the need for coordinate wrapping, we selected a 1 × 1 graphene unit in the center of the supercell, where the molecule is translated along the vector b = [18.485, 10.672, 0]. The (x, y) coordinates of E2 were thus computed as (a_1 * X, a_2 * Y), where X, $Y \epsilon$ [0, 1]. The molecular in-plane rotation was implemented 360° counterclockwise from the x-axis γ = 0 position. Lattice vectors, location of the 1 × 1 graphene unit on the graphene supercell, and search boundaries are described in Figure 3a.

According to previous adsorption studies, the z-coordinate has a weak effect on the variation in the energy landscape when adsorption is dominated by vdW forces. However, it does affect the interaction magnitude. To find the molecule height range that maximizes the interaction, we performed a 1D BOSS search where we only allowed the algorithm to alter the height of the molecule. The nonperiodic radial basis function (rbf) kernel was used, and the bounds were set to $z \epsilon$ [3, 7] (Å). The estimated range for the objective function was set to [−2, −1] (eV). We used 5 initial points and iterated 15 new points. Based on the results (Figure 3b), we fixed the z-coordinate to 4 Å and performed the main structure search with the remaining three degrees of freedom: 2D translation of the molecule on the graphene sheet ($x-y$ translation) and in-

https://doi.org/10.1021/acsomega.4c03485
ACS Omega 2024, 9, 34684−34691

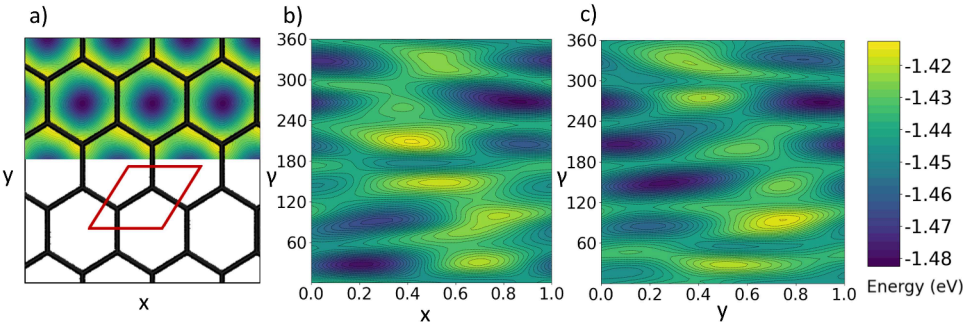

Figure 4. 2D cross sections of the adsorption energy landscape after the 300th BOSS iteration. (a) Repeated $x-y$ cross section overlapped with the graphene sheet. The red rhombus indicates the location of a single unit cell on the graphene supercell. (b) $x-\gamma$ cross section. (c) $y-\gamma$ cross section. The same energy scale applies to all subfigures.

place rotation of the molecule around the z-axis perpendicular to the surface.

We used Python scripts to interface the BOSS code with the FHI-aims simulations. Each iteration followed a workflow where we (1) determined the next sampling location using BOSS, (2) utilized ASE (Atomic Simulation Environment)[36] to manipulate the E2 coordinates accordingly, (3) performed a single-point FHI-aims DFT calculation, (4) extracted the adsorption energy of the studied configuration, and (5) updated our 3D model for adsorption energy. In the 3D BOSS simulations, we used the standard periodic kernel for each dimension, with periods 1, 1 and 360, and multiplied them into one product kernel. The model was initialized with 5 Sobol points and updated with 300 new points selected by the eLBC acquisition function.[37,38] To make sure all local minima had converged after 300 iterations, we output the local minima every 50 new iterations by applying the Broyden–Fletcher–Goldfarb–Shanno algorithms[39] to the 3D adsorption energy surrogate model, following previously established methodology.[22]

Refinement and Analysis. Output of the local minimizers at the 300th iteration was used to analyze the adsorption energy landscape. Our goal was to identify the stable and unique local minima with low adsorption energy. Due to the 60° rotational periodicity of graphene, we discarded all local minima structures that could be constructed by 60° rotations of lower energy minimum configurations. We also excluded from further considerations such variants of the high-symmetry configurations that are near in energy because they are likely artifacts originating from energy fluctuations in the surrogate model.

Next, we removed the rigid BB approximations and performed two consecutive DFT relaxations of the chosen minimum configurations, one with light and the other one with tight settings. Only one carbon atom in the coordinate origin of the graphene sheet remained fixed to prevent translational drift. Then, we studied the structural features, such as graphene corrugation and E2 deformation, and the electronic structure, such as DOS and charge transfer, of the chosen minimum configurations. The purpose of the DOS calculations was to explore the shape of molecular states before and after adsorption and discover whether the nature of the adsorption was chemical (via covalent bonds) or physical (via dispersion).

RESULTS

The 3D adsorption structure search for E2 molecules on pristine graphene produced a well-converged surrogate model for the adsorption interaction. Figure 4 displays 2D cross sections of the final adsorption energy landscape in $x-y$, $x-\gamma$, and $y-\gamma$. It illustrates that there is only one minimum in the $x-y$ plane, located at the hollow site of the graphene lattice. However, we observed repeated minima every 60° in the γ-variable, reflecting the presence of many similar local minimum structures—this is expected given the symmetry of the graphene substrate.

After pruning for duplicates, we obtained two unique low-energy local minimum configurations E2-A and E2-B, illustrated in Figure 5. Structure A was positioned above the

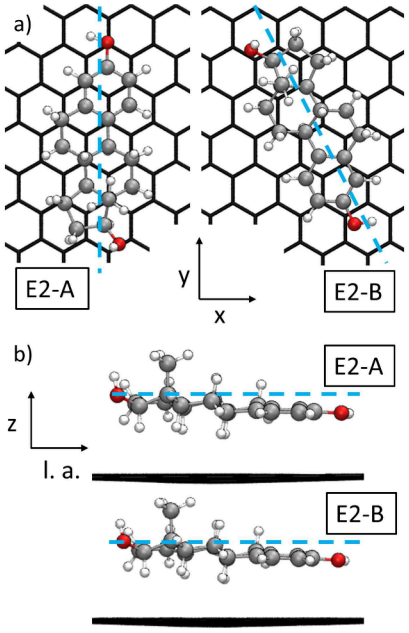

Figure 5. Refined minimum structures E2-A and E2-B in (a) top-view and (b) side-view. The dashed lines denote the long axis of the molecule.

hollow site, with the molecular long axis oriented along the graphene armchair [010] surface direction. Structure B was above the bridge site, with its long axis rotated 30° with respect to structure A, along the graphene zigzag bonds. We note that in the E2-A configuration, a graphene C atom is positioned directly under each ring structure of the molecule, while for the E2-B structure no distinct features were observed. In the BOSS surrogate model for adsorption, these structures were very close in adsorption energy: −1.48 eV (E2-A) and −1.45 eV

https://doi.org/10.1021/acsomega.4c03485
ACS Omega 2024, 9, 34684−34691

(E2-B). After full structural refinement, the final adsorption energies were −1.56 eV (E2-A) and −1.53 eV (E2-B). Throughout the relaxations, the initial energy difference of only 0.03 eV between the structures E2-A and E2-B was maintained, with E2-A consistently emerging as the global minimum configuration. Information on the energetics and structural features is summarized in Table 1.

Table 1. Coordinates of the Minimum Structures (x, y, γ), Adsorption Energy E_{ADS}, Induced Graphene Corrugation Δz_{GR}, Molecule Height h, Change in Height of the Whole Molecule Δz_{E2} and of its Phenolic Oxygen Δz_O, and the Mulliken Charge Transfer Δq

property	E2-A	E2-B
(x, y, γ)	(0.87, 0.91, 268)	(0.39, 0.69, 117)
E_{ADS} (eV)	−1.56	−1.53
Δz_{GR} (Å)	0.32	0.31
h (Å)	3.84	3.88
Δz_{E2} (Å)	0.34	0.31
Δz_O (Å)	1.06	1.11
Δq (e)	10×10^{-3}	10×10^{-6}

Next, we reviewed the structural changes that the molecule and the surface experience upon adsorption. Figure 5 illustrates that the two structural configurations have very similar features.

At the molecular adsorption site, we observed a graphene indentation (Δz_{GR}), where the sides of the sheet shift up and the center of the sheet shifts down in z. The maximum graphene corrugation was similar in both cases: 0.32 Å for E2-A and 0.31 Å for E2-B. Since the 3D BOSS search was carried out with the molecule at a fixed height of z = 4 Å, the relaxation caused the molecule to approach the substrate by approximately 0.3 Å. However, there were no noticeable changes in x, y, or γ, indicating that the height constraint of the structure search did not affect the accuracy of the final result. The final heights of the adsorbed molecules were 3.84 Å (E2-A) and 3.88 Å (E2-B), measuring from the lowest atom of graphene to the COM of E2. During optimization, the largest E2 structural change involved the phenolic O atom at one end of the molecule lowering toward the surface by approximately 1.1 Å. This caused the molecular backbone to flatten in comparison to the gas phase structure in Figure 2. It is noteworthy that the structural properties of E2-A and E2-B configurations always differed by less than 0.1 Å, further pointing to strong similarity.

Lastly, we shifted our attention to the electronic structure properties of the two configurations and found them nearly identical. For simplicity, we proceed to discuss the properties of the E2-A structure only. Figure 6 illustrates the total DOS of the adsorbed system and the pDOS contribution of the E2 molecule. The Dirac cone of graphene clearly dominates the system DOS at the Fermi level. E2 molecular HOMO and LUMO levels remain inside the valence and conduction band respectively, with HOMO positioned about −1.0 eV below the Fermi level. In comparison with the DOS states of gas phase E2, we found the pDOS states of adsorbed E2 to be similarly narrow, with no evidence of hybridization. Moreover, the E2 HOMO−LUMO gap and the differences between different electronic states appear entirely unchanged by adsorption. All evidence points to dispersion as the main bonding mechanism and absence of covalent bonding.

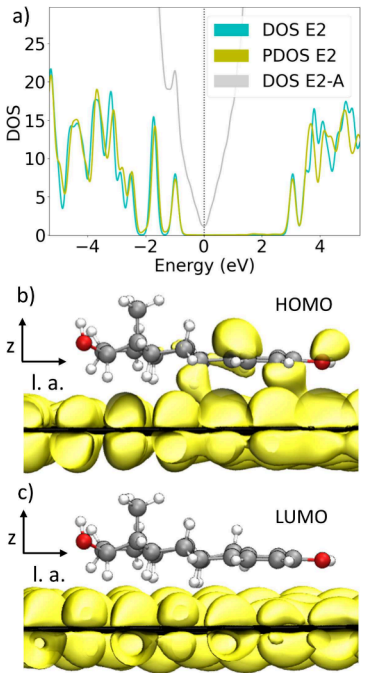

Figure 6. Electronic structure of E2-A. (a) Total DOS of E2-A and isolated E2; pDOS contribution of E2 to the total DOS of E2-A. The total DOS plot of isolated E2 has been shifted by 2.19 eV to enable comparison with the E2 pDOS plot. (b) HOMO and (c) LUMO of E2-A with 0.01 e/Å^3. The horizontal axis corresponds to the long axis of the refined molecule.

To gain further insight into the adsorption mechanisms, we investigated the DOS states associated with the HOMO and LUMO orbitals of adsorbed E2-A. The results are shown in Figures 6b and 6c. In contrast to the LUMO state, the E2 HOMO orbital exhibits partial overlap with the surface states of graphene. The aromatic half of the molecule that terminates in the phenolic O appears to share states with the surface, which might explain the adsorption-induced structural changes in this part of the molecule. We carried out Mulliken charge analysis to compute molecule−surface charge transfer Δq. With less than 0.001 e, there is effectively no charge transfer in this system, which further suggests molecular physisorption.

DISCUSSION

In this study, we applied BO-guided autonomous structure search to identify the optimal adsorption configurations of E2 on a graphene-sensing substrate. The main advantages of autonomous structure search are lack of human bias in structural sampling and the comprehensive sampling to ensure all relevant solutions are found. Nevertheless, we did integrate expert knowledge into the model at the outset, when selecting the degrees of freedom. We excluded molecular tilting and carried out the search with the molecular backbone parallel to the surface. This simplification of the search space was motivated by the strong electronic conjugation of both the molecule and substrate, where $\pi-\pi$ stacking interactions favor parallel planar geometries. Our results agree with previous observations in literature, where horizontal (parallel) E2 adsorbate configurations on similar substrates were found to be energetically favored over vertical (perpendicular) adsorbates.[17,18]

We also simplified the search by maintaining the molecule and surface as rigid building blocks during sampling. In the

https://doi.org/10.1021/acsomega.4c03485
ACS Omega 2024, 9, 34684−34691

case of conjugated materials like E2 and graphene, such approximations work well, as revealed by the very small 0.1 eV lowering in energy during full relaxation. The small shift in energy is associated with the overall slight lowering of E2 toward the surface (by 0.3 Å) and the downward shift in the phenolic end-group (by 1.1 Å).

The structure search revealed two distinct adsorbate configurations, E2-A and E2-B. The structures are very close in energy and have very similar structural features (molecule shape, adsorption height) but differ in the orientation with respect to the substrate. We also note that in Figure 4 the adsorption energy landscape is flat, with an energy corrugation of only 0.06 eV. This value is comparable to the average thermal energy accessible at room temperature, so the molecule might easily be able to overcome the barriers between the different energy minima. This leads us to conclude that E2 is unlikely to be anchored to the substrate in the two low-lying minima configurations. Instead, it is probable that the molecule is diffusing across pristine graphene, occupying multiple local minima in turn. Such adsorption scenarios are typical for conjugated systems adsorbed to pristine graphene.[30]

The electronic structure of the adsorbed molecule, such as pDOS and charge transfer, revealed no hybridization by the substrate. All evidence points to physisorption as the main bonding mechanism, as found in previous studies.[17] These findings are reasonable, given the inert nature of unmodified graphene and the absence of strongly reactive E2 functional groups. To explore the effect of implicit solvent on bonding strength, we fixed adsorbate configurations and recomputed adsorption energies in implicit water to find little change (up to 0.15 eV).[40−44]

Currently, there exists a large gap between the experimental reality and theoretical simulations. While our results agree with the literature, this simple sensor model has limited use in clarification of experimental sensing. The calculations were performed in vacuum and in the presence of implicit solvent, which does not fully reflect the real-world environment. Furthermore, we do not account for pH, the presence of explicit solvent or other solvated compounds, or the impact of applying potential to the interface in electrochemical measurements. Thus, the results presented here should not be extrapolated into experimental research without thorough consideration.

By carefully extending our simulations to consider more and more aspects of the real-world environment, we strive to narrow the gap between experiments and simulations. Eventually, the goal should be to develop the ability to screen for the most promising sensing substrates computationally instead of experimental trial-and-error methods. Interesting functionalities include modified graphene surfaces and different carbon nanotube chiralities.

This study demonstrates the potential of autonomous AI-guided structure search for sensor materials. Nowadays, the development of carbon-based sensors focuses on complex carbonaceous materials, such as glassy carbon and doped or hybrid carbon nanomaterials. With such complex substrates, there is a risk of some important adsorption minima candidates being left out due to human bias in simulations. As the development of substrate materials advances, it will be even more central that we can find all possible adsorption configurations using automated structure search tools.

By integrating both experimental and computational findings, we can deepen our understanding of electrochemical interfaces. The insight from atomistic models can be strategically employed to customize an optimal response for measuring targeted analytes. This approach facilitates a data-driven and rational design of sensor materials, allowing for customized tailoring to specific applications. The potential for advancing sensor design beyond the current state-of-the-art is significant.

CONCLUSIONS

In this Article, our objectives were to identify the stable adsorption minima of E2 on pristine graphene and identify the nature of the bonding interactions. We combined Bayesian optimization with DFT to carry out configurational sampling and identify lowest energy adsorbates. We detected two distinct local minima structures with very similar adsorption energies but different orientations with respect to the substrate. The low energy barriers for surface diffusion suggest that at room temperature, E2 would switch between these configurations and other symmetry-equivalent ones. Our electronic structure analysis confirmed that E2 physisorbs to pristine graphene. Further studies are needed to explore the interactions between E2 and modified graphene-based surfaces and to consider the factors of the real world that were not considered here.

This study demonstrates that Bayesian optimization provides a relatively fast and more systematic alternative for performing adsorption structure search on only a few expert-chosen candidate structures. There is no doubt that computational simulations play an essential and growing role in the field of electrochemical sensing. At their best, they can identify trends in the interactions between sensing substrates and target molecules. This can eventually accelerate the development and commercialization of novel sensor materials and sensing platforms.

AUTHOR INFORMATION

Corresponding Authors

Milica Todorović − *Department of Mechanical and Materials Engineering, University of Turku, Turku 20500, Finland;* orcid.org/0000-0003-0028-0105; Phone: +358 29 450 3619; Email: milica.todorovic@utu.fi

Emilia Peltola − *Department of Mechanical and Materials Engineering, University of Turku, Turku 20500, Finland;* orcid.org/0000-0002-8868-9273; Phone: +358 29 450 4706; Email: emilia.peltola@utu.fi

Author

Saara Sippola − *Department of Mechanical and Materials Engineering, University of Turku, Turku 20500, Finland;* orcid.org/0009-0002-6673-0201

Complete contact information is available at: https://pubs.acs.org/10.1021/acsomega.4c03485

Notes

The authors declare no competing financial interest.

ACKNOWLEDGMENTS

The authors wish to acknowledge CSC−IT Center for Science, Finland, for generous computational resources. This research has been supported by the Research Council of Finland (grant #347021). The work was conducted under the #SUSMAT umbrella.

REFERENCES

(1) Lu, Y.; Sareddy, G. R.; Wang, J.; Wang, R.; Li, Y.; Dong, Y.; Zhang, Q.; Liu, J.; O'Connor, J. C.; Xu, J.; Vadlamudi, R. K.; Brann, D. W. Neuron-Derived Estrogen Regulates Synaptic Plasticity and Memory. *J. Neurosci.* **2019**, *39*, 2792−2809.

(2) Taxier, L. R.; Gross, K. S.; Frick, K. M. Oestradiol as a neuromodulator of learning and memory. *Nat. Rev. Neurosci.* **2020**, *21*, 535−550.

(3) Remage-Healey, L.; Maidment, N. T.; Schlinger, B. A. Forebrain steroid levels fluctuate rapidly during social interactions. *Nature Neuroscience* **2008**, *11*, 1327−1334.

(4) Tiedeken, E. J.; Tahar, A.; McHugh, B.; Rowan, N. J. Monitoring, sources, receptors, and control measures for three European Union watch list substances of emerging concern in receiving waters − A 20year systematic review. *Science of The Total Environment* **2017**, *574*, 1140−1163.

(5) Barreiros, L.; Queiroz, J. F.; Magalhães, L. M.; Silva, A. M. T.; Segundo, M. A. Analysis of 17-β-estradiol and 17-α-ethinylestradiol in biological and environmental matrices — A review. *Microchemical Journal* **2016**, *126*, 243−262.

(6) Schiebinger, L. Women's health and clinical trials. *J. Clin. Invest.* **2003**, *112*, 973−977.

(7) Hendriksen, L. C.; van der Linden, P. D.; Lagro-Janssen, A. L. M.; van den Bemt, P. M. L. A.; Siiskonen, S. J.; Teichert, M.; Kuiper, J. G.; Herings, R. M. C.; Stricker, B. H.; Visser, L. E. Sex differences associated with adverse drug reactions resulting in hospital admissions. *Biol. Sex Differ.* **2021**, *12*, 34.

(8) Wang, J.; Sareddy, G. R.; Lu, Y.; Pratap, U. P.; Tang, F.; Greene, K. M.; Meyre, P. L.; Tekmal, R. R.; Vadlamudi, R. K.; Brann, D. W. Astrocyte-Derived Estrogen Regulates Reactive Astrogliosis and is Neuroprotective following Ischemic Brain Injury. *Journal of Neuroscience: The Official Journal of the Society for Neuroscience* **2020**, *40*, 9751−9771.

(9) European Commission. COM(2011) 876 Final. Proposal for a Directive of the European Parliament and of the Council Amending Directives 2000/60/EC and 2008/105/ EC as Regards Priority Substances in the Field of Water Policy. Brussels, 2011.

(10) Rosner, W.; Hankinson, S. E.; Sluss, P. M.; Vesper, H. W.; Wierman, M. E. Challenges to the Measurement of Estradiol: An Endocrine Society Position Statement. *Journal of Clinical Endocrinology & Metabolism* **2013**, *98*, 1376−1387.

(11) Weese-Myers, M. E.; Ross, A. E. Electrochemical characterization of 17β-estradiol with fast-scan cyclic voltammetry. *Electroanalysis* **2023**, *35*, e202200560.

(12) Regasa, M. B.; Nyokong, T. Design and fabrication of electrochemical sensor based on molecularly imprinted polymer loaded onto silver nanoparticles for the detection of 17-β-estradiol. *J. Mol. Recog.* **2022**, *35*, e2978.

(13) Masikini, M.; Ghica, M. E.; Baker, P. G. L.; Iwuoha, E. I.; Brett, C. M. A. Electrochemical Sensor Based on Multi-walled Carbon Nanotube/Gold Nanoparticle Modified Glassy Carbon Electrode for Detection of Estradiol in Environmental Samples. *Electroanalysis* **2019**, *31*, 1925−1933.

(14) Janegitz, B. C.; dos Santos, F. A.; Faria, R. C.; Zucolotto, V. Electrochemical determination of estradiol using a thin film containing reduced graphene oxide and dihexadecylphosphate. *Materials Science and Engineering: C* **2014**, *37*, 14−19.

(15) Sainio, S.; Leppänen, E.; Mynttinen, E.; Palomäki, T.; Wester, N.; Etula, J.; Isoaho, N.; Peltola, E.; Koehne, J.; Meyyappan, M.; Koskinen, J.; Laurila, T. Integrating Carbon Nanomaterials with Metals for Bio-sensing Applications. *Molecular Neurobiology* **2020**, *57*, 179−190.

(16) Jiang, L.-h.; Liu, Y.-g.; Zeng, G.-m.; Xiao, F.-y.; Hu, X.-j.; Hu, X.; Wang, H.; Li, T.-t.; Zhou, L.; Tan, X.-f Removal of 17β-estradiol by few-layered graphene oxide nanosheets from aqueous solutions: External influence and adsorption mechanism. *Chemical Engineering Journal* **2016**, *284*, 93−102.

(17) Abraham, B. M.; Parey, V.; Jyothirmai, M. V.; Singh, J. K. Tuning the structural properties and chemical activities of graphene and hexagonal boron nitride for efficient adsorption of steroidal pollutants. *Appl. Surf. Sci.* **2022**, *580*, 152110.

(18) de Oliveira, P. V.; Zanella, I.; Bulhões, L. O. S.; Fagan, S. B. Adsorption of 17 β- estradiol in graphene oxide through the competing methanol co-solvent: Experimental and computational analysis. *J. Mol. Liq.* **2021**, *321*, 114738.

(19) Borthakur, P.; Boruah, P. K.; Das, M. R.; Kulik, N.; Minofar, B. Adsorption of 17α-ethynyl estradiol and β-estradiol on graphene oxide surface: An experimental and computational study. *J. Mol. Liq.* **2018**, *269*, 160−168.

(20) Todorović, M.; Gutmann, M. U.; Corander, J.; Rinke, P. Bayesian inference of atomistic structure in functional materials. *npj Comput. Mater.* **2019**, *5*, 1−7.

(21) BOSS. BOSS 1.9.0 documentation. https://cest-group.gitlab.io/boss/.

(22) Järvi, J.; Rinke, P.; Todorović, M. Detecting stable adsorbates of (1S)-camphor on Cu(111) with Bayesian optimization. *Beilstein Journal of Nanotechnology* **2020**, *11*, 1577−1589.

(23) Järvi, J.; Alldritt, B.; Krejčí, O.; Todorović, M.; Liljeroth, P.; Rinke, P. Integrating Bayesian Inference with Scanning Probe Experiments for Robust Identification of Surface Adsorbate Configurations. *Adv. Funct. Mater.* **2021**, *31*, 2010853.

(24) Egger, A. T.; Hörmann, L.; Jeindl, A.; Scherbela, M.; Obersteiner, V.; Todorović, M.; Rinke, P.; Hofmann, O. T. Charge Transfer into Organic Thin Films: A Deeper Insight through Machine-Learning-Assisted Structure Search. *Adv. Sci.* **2020**, *7*, 2000992.

(25) Blum, V.; Gehrke, R.; Hanke, F.; Havu, P.; Havu, V.; Ren, X.; Reuter, K.; Scheffler, M. Ab initio molecular simulations with numeric atom-centered orbitals. *Comput. Phys. Commun.* **2009**, *180*, 2175−2196.

(26) Perdew, J. P.; Burke, K.; Ernzerhof, M. Generalized Gradient Approximation Made Simple. *Phys. Rev. Lett.* **1996**, *77*, 3865−3868.

(27) Tkatchenko, A.; Scheffler, M. Accurate Molecular Van Der Waals Interactions from Ground-State Electron Density and Free-Atom Reference Data. *Phys. Rev. Lett.* **2009**, *102*, 073005.

(28) Avogadro: An open-source molecular builder and visualization tool. http://avogadro.cc/.

(29) Hanwell, M. D.; Curtis, D. E.; Lonie, D. C.; Vandermeersch, T.; Zurek, E.; Hutchison, G. R. Avogadro: an advanced semantic chemical editor, visualization, and analysis platform. *J. Cheminf.* **2012**, *4*, 17.

(30) Järvi, J.; Todorović, M.; Rinke, P. Efficient modeling of organic adsorbates on oxygen-intercalated graphene on Ir(111). *Phys. Rev. B* **2022**, *105*, 195304.

(31) Cooper, D. R.; D'Anjou, B.; Ghattamaneni, N.; Harack, B.; Hilke, M.; Horth, A.; Majlis, N.; Massicotte, M.; Vandsburger, L.; Whiteway, E.; Yu, V. Experimental Review of Graphene. *ISRN Condensed Matter Physics* **2012**, *2012*, 1−56.

(32) Garcia, A. G.; Baltazar, S. E.; Castro, A. H. R.; Robles, J. F. P.; Rubio, A. Influence of S and P Doping in a Graphene Sheet. *J. Comput. Theor. Nanosci.* **2008**, *5*, 2221−2229.

(33) Chakarova-Käck, S. D.; Schröder, E.; Lundqvist, B. I.; Langreth, D. C. Application of van der Waals Density Functional to an Extended System: Adsorption of Benzene and Naphthalene on Graphite. *Phys. Rev. Lett.* **2006**, *96*, 146107.

(34) Otyepková, E.; Lazar, P.; Cépe, K.; Tomanec, O.; Otyepka, M. Organic adsorbates have higher affinities to fluorographene than to graphene. *Appl. Mater. Today* **2016**, *5*, 142−149.

(35) Behan, J. A.; Hoque, M. K.; Stamatin, S. N.; Perova, T. S.; Vilella-Arribas, L.; García-Melchor, M.; Colavita, P. E. Experimental and Computational Study of Dopamine as an Electrochemical Probe of the Surface Nanostructure of Graphitized N-Doped Carbon. *J. Phys. Chem. C* **2018**, *122*, 20763−20773.

(36) Larsen, A. H.; et al. The atomic simulation environment—a Python library for working with atoms. *J. Phys.: Condens. Matter* **2017**, *29*, 273002.

(37) Srinivas, N.; Krause, A.; Kakade, S. M.; Seeger, M. Gaussian Process Optimization in the Bandit Setting: No Regret and

https://doi.org/10.1021/acsomega.4c03485
ACS Omega 2024, 9, 34684−34691

Experimental Design. *IEEE Transactions on Information Theory* **2012**, *58*, 3250−3265.
(38) Brochu, E.; Cora, V. M.; de Freitas, N. A Tutorial on Bayesian Optimization of Expensive Cost Functions, with Application to Active User Modeling and Hierarchical Reinforcement Learning. 2010; http://arxiv.org/abs/1012.2599.
(39) Byrd, R. H.; Lu, P.; Nocedal, J.; Zhu, C. A Limited Memory Algorithm for Bound Constrained Optimization. *SIAM J. Sci. Comput.* **1995**, *16*, 1190.
(40) Filser, J.; Reuter, K.; Oberhofer, H. Piecewise multipole-expansion implicit solvation for arbitrarily shaped molecular solutes. *J. Chem. Theory Comput.* **2022**, *18*, 461−478.
(41) Sinstein, M.; Scheurer, C.; Matera, S.; Blum, V.; Reuter, K.; Oberhofer, H. Efficient implicit solvation method for full potential DFT. *J. Chem. Theory Comput.* **2017**, *13*, 5582−5603.
(42) Havu, V.; Blum, V.; Havu, P.; Scheffler, M. Efficient O (N) integration for all-electron electronic structure calculation using numeric basis functions. *J. Comput. Phys.* **2009**, *228*, 8367−8379.
(43) Yu, V. W.-z.; Corsetti, F.; García, A.; Huhn, W. P.; Jacquelin, M.; Jia, W.; Lange, B.; Lin, L.; Lu, J.; Mi, W.; et al. ELSI: A unified software interface for Kohn−Sham electronic structure solvers. *Comput. Phys. Commun.* **2018**, *222*, 267−285.
(44) Rycroft, C. A three-dimensional Voronoi cell library in C++. *Chaos* **2009**, *19*, 041111.

https://doi.org/10.1021/acsomega.4c03485
ACS Omega 2024, 9, 34684−34691